Available online at www.sciencedirect.com
SCIENCE DIRECT
Polymer 45 (2004) 6897–6908
polymer
www.elsevier.com/locate/polymer

Thermal and dielectric properties and curing kinetics of nanomaterials formed from poss-epoxy and meta-phenylenediamine

Wen-Yi Chen[a], Yen-Zen Wang[b], Shiao-Wei Kuo[a], Chih-Feng Huang[a], Pao-Hsiang Tung[a], Feng-Chih Chang[a,*]

[a]*Institute of Applied Chemistry, National Chiao Tung University, Hsinchu, 30050, Taiwan, ROC*
[b]*Department of Chemical Engineering, National Yun-Lin University of Science and Technology, 640, Yun-Lin, Taiwan, ROC*

Received 2 February 2004; received in revised form 17 June 2004; accepted 29 July 2004
Available online 20 August 2004

Abstract

A nanoporous polyhedral oligomeric silisesquioxane (POSS) containing eight epoxy functional groups [octakis(dimethylsiloxypropylglycidyl ether)silsesquioxane, OG] reacts with meta-phenylenediamine (mPDA) to form epoxy resin network with nanostructures. The glass transition temperature (T_g) of the cured OG/mPDA product is significantly higher than that of the diglycidyl ether of bisphenol A (DGEBA) cured with mPDA (DGEBA/mPDA) material due to the presence of the POSS cages that is able to effectively hinder the motion of the network junctions. The cured OG/mPDA product inherently possesses higher thermal stability than the cured DGEBA/mPDA product based on higher maximum decomposition rate temperature, and higher char yield of the former. However, the existence of large fraction of the unreacted amine groups causes lower initial decomposition temperature of the OG/mPDA because it tends to decompose or volatilize on heating at relatively low temperature. The dielectric constant of the OG/mPDA material (2.31) is substantially lower than that of the DGEBA/mPDA (3.51) as a consequence the presence of nanoporous POSS cubes in the epoxy matrix.

Keywords: POSS; Epoxy resin; Curing kinetics

1. Introduction

Hybrid materials having both inorganic and organic components are interesting substances from the standpoint of their potentially increased performance capabilities relative to those of either of their nonhybrid species. The polyhedral oligomeric silsesquioxanes (POSS) have received a great deal of attention recently as modifiers of organic polymers. One special feature of the POSS particle is that its dimension (1.5 nm) is of comparable size to that of typical polymer segments. Incorporation of POSS particles into linear thermoplastics or thermoset networks is able to improve their thermal, oxidative, and dimensional stability and this process provides many polymer resins for high-performance engineering applications. Some examples of thermoplastic and thermoset systems have undergone such modification including methacrylates [1,2], styrenes [3], norbornenes [4], epoxies [5–10], and siloxanes [11] etc. Clearly, many nanocomposites can be designed using functionalized POSS derivatives in conjunction with traditional plastics and resins. It has been reported that monofunctional or multifunctional POSS-epoxies can be incorporated into the backbone of epoxy resin to improve its thermal properties [5–10].

In this investigation, we synthesized a multifunctional POSS-epoxy monomer that was then reacted with mPDA to form epoxy based nanomaterials. Specifically, we focused our attention in this study on the curing kinetics and thermal and dielectric properties of the POSS-containing materials by differential scanning calorimetry (DSC), modulated differential scanning calorimetry (MDSC), thermogravimetric analysis (TGA), and dielectric analysis (DEA).

* Corresponding author. Tel.: +886-3-5727077; fax: +886-3-5719507.
E-mail addresses: kuosw@cc.nctu.edu.tw (S.-W. Kuo), changfc@-mail.nctu.edu.tw (F.-C. Chang).

0032-3861/$ - see front matter © 2004 Elsevier Ltd. All rights reserved.
doi:10.1016/j.polymer.2004.07.070

2. Experimental

2.1. Materials

Octakis(dimethylsilyloxy)silsesquixoxane ($HMe_2SiOSiO_{1.5})_8$ and platinum 1,3-divinyl-1,1,3,3-tetramethyldisiloxane [Pt(dvs)] were purchased from the Aldrich, USA. Allyl glycidyl ether (AGE) and meta-phenylenediamine (mPDA) were purchased from Acros, Belgium. The DGEBA (DER 331, EEW = 190 g/equiv.) was purchased from Dow Chemical Company of USA. The chemical structures of the compounds used in this study are depicted in Scheme 1.

2.2. Sample preparations

2.2.1. Octakis(dimethylsilyloxypropylglycidyl ether)silsesquioxane (OG) [6]

The synthesis of OG is presented in Scheme 2. The POSS derivative $(HMe_2SiOSiO_{1.5})_8$ (0.50 g, 0.49 mmol) and toluene (5 ml) were added into a 25 ml Schlenk flask and stirred magnetically. AGE (0.46 ml, 3.92 mmol) was added, followed by 10 drops of 2.0 mM Pt(dvs). The reaction mixture was stirred for 8 h at 80 °C, cooled, and then dry activated charcoal was added. After stirring for 10 min, the mixture was filtered through a 0.45 μm Teflon membrane. The

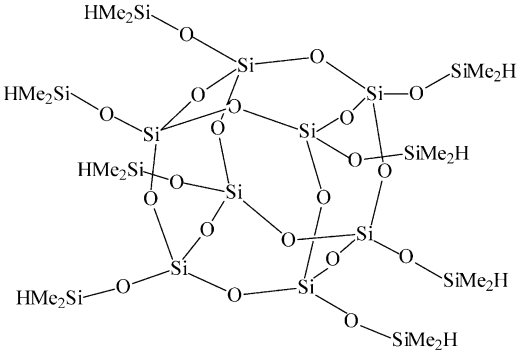

(A) POSS

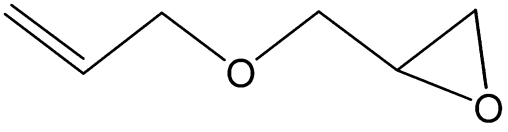

(B) AGE

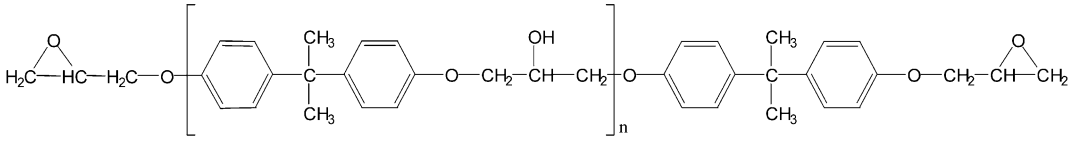

(C) DGEBA

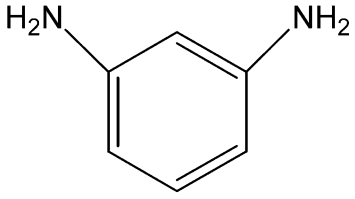

(D) mPDA

Scheme 1. Chemical structures of the compounds used in this study.

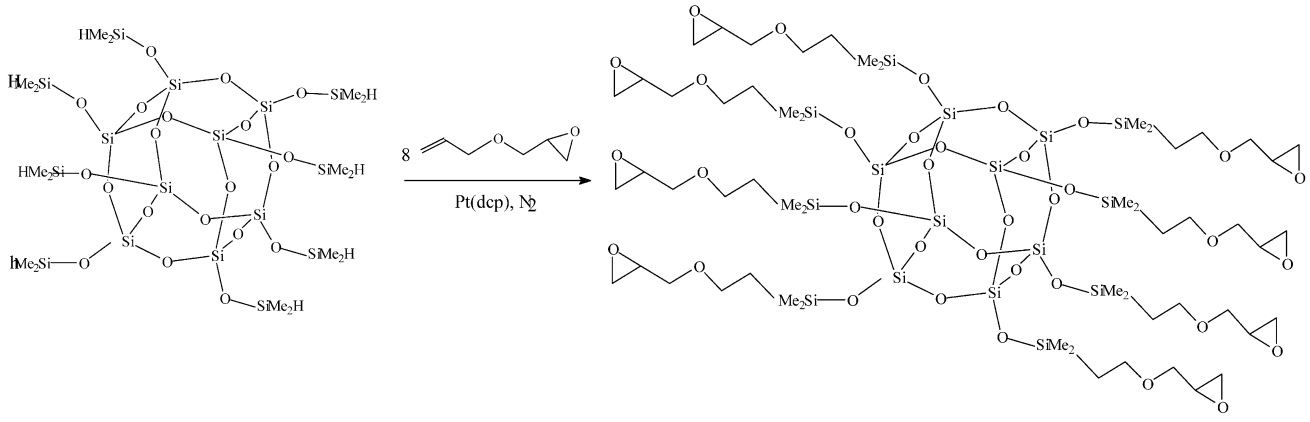

Scheme 2. Synthesis of OG.

solvent was evaporated and an opaque viscous liquid was obtained (0.86 g, 90% yield).

2.3. Preparing cured samples

2.3.1. OG/mPDA system

Stoichiometric amounts of OG and mPDA monomers were mixed in a high-speed stirrer for 10 min at 55 °C. After degassing under vacuum, the mixture was cured at 120 °C for 180 min (pre-cured) and then at 190 °C for 100 min (post-cured) before thermal and dielectric characterizations.

2.3.2. DGEBA/mPDA system

Stoichiometric amounts of DGEBA and mPDA monomers were mixed in a high-speed stirrer for 10 min at 55 °C. After degassing under vacuum, the mixture was cured at 120 °C for 180 min (pre-cured) and then at 190 °C for 100 min (post-cured) before thermal and dielectric characterizations.

2.4. Dynamic curing kinetics

The dynamic curing kinetics was studied using a Du-Pont 2910 Differential Scanning Calorimeter operating under a nitrogen atmosphere. The sample (ca. 7 mg) was placed in a sealed aluminum sample pan. Dynamic curing scan were conducted from 30 to 350 °C at a heating rate of 10, 20, 30 or 40 °C/min.

2.5. Isothermal curing kinetics

Isothermal curing was conducted at four different temperatures (90, 100, 110 and 120 °C).

2.6. Characterization

2.6.1. Fourier transform infrared spectra (FT-IR)

To analyze the epoxide content of the system, each sample was placed on a KBr pellet and FTIR spectra were obtained at 120 and 190 °C using a Nicolet AVATAR 320 FT-IR spectrometer (Madison, Wisconsin, USA) operating at a resolution of 2 cm^{-1}.

2.6.2. ^{13}C NMR spectra

All solutions were prepared by dissolving samples in $CDCl_3$. ^{13}C spectra were recorded at 25.8 °C on a Varian Unity 400 spectrometer. Spectral parameters used a spectral width of 21,200 Hz, a 908 pulse width of 7.2 ms, a filter bandwidth of 21,000 Hz, an acquisition time of 0.9 s and 2500 repetitions.

2.6.3. Solid-state NMR spectra

High-resolution solid-state ^{13}C NMR experiments were carried out at room temperature using a Bruker DSX-400 spectrometer (Bruker Instruments, Billerica, MA) operated at resonance frequencies of 399.53–100.47 and 399.53–161.72 MHz for ^{13}C. The ^{13}C CP/MAS spectra were measured with a 3.9 μs 90° pulse, with 3 s pulse delay time, acquisition time of 30 ms, and 2048 scans. All NMR spectra were taken at 300 K using broadband proton decoupling and normal cross-polarization pulse sequencing. A magic angle sample spinning (MAS) rate of 5.4 kHz was used to eliminate resonance broadening attributed to the anisotropy of the chemical shift tensors.

2.6.4. Modulated differential scanning calorimetry (MDSC)

Glass transition temperatures were determined using a Du-Pont Q100 Modulated Differential Scanning Calorimeter operating under nitrogen atmosphere. The cured sample (ca. 7 mg) was placed in a sealed aluminum sample pan and was heated from 30 to 300 °C at heating rate of a 5 °C/min using an amplitude of modulation ± 0.6 °C and a period of 60 s.

2.6.5. Dynamic mechanical analysis (DMA)

Dynamic mechanical behavior of cured sample was studied using a Du-Pont 2980 dynamic mechanical analyzer. Cured sample was polished to $\approx 3.0 \times 13.0 \times 30.0$ mm^3 and mounted on a single cantilever clamp. The

mechanical properties were measured under nitrogen in step mode every 5 °C from 100 to 350 °C at frequency $r = 1$ Hz.

2.6.6. Thermogravimetric analysis (TGA)

The thermal stability of the samples was characterized by using a Du-Pont 2050 Thermogravimetric Analyzer operating under a nitrogen atmosphere. The cured sample ca. 7 mg was placed in a Pt cell and heated at a rate of 20 °C/min from 30 to 800 °C at a nitrogen flow rate of 60 ml/min.

2.6.7. Dielectric analysis (DEA)

DEA experiments were performed using a Du-Pont 2970 Dielectric Analyzer equipped with a ceramic parallel plate sensor. The frequency used for the DEA experiments was 100 kHz and the permittivity (ε') was monitored.

3. Results and discussion

An optimal curing process depends on the understanding of the curing kinetics, curing mechanism, and an accurate modeling of the curing process. This modeling process includes determining the mechanism and an appropriate kinetic equation in terms of reaction order and activation energy. An accurate model not only helps to predict the curing behavior and assist process design and control, but also can be used to predict aging and degradation of thermosetting polymer systems. The model can further be used to compare the curing behavior of different systems or formulations using different matrices, catalysts, fillers and additives.

The current understanding of the mechanism and kinetics of curing lags the rapid increase in formulations and industrial applications of epoxy-based resins and composite systems. The mechanism and kinetics of curing have yet to be understood comprehensively, and an accurate model of an optimal curing process has yet to be clearly established [11]. To date, no study has been reported that models the curing of the OG/mPDA system.

An appropriate method must be used to measure accurately the curing kinetic parameters, namely the degree of conversion (α), the conversion rate ($d\alpha/dt$), and the activation energy (E).

The rate of conversion can be defined as follow:

$$\frac{d\alpha}{dt} = \frac{dH/dt}{\Delta H_{Rxn}} \tag{1}$$

where ΔH_{Rxn} is the heat of reaction. DSC techniques can be applied to this problem using two basic approaches: isothermal curing carried out at a single cure temperature and dynamic curing undertaken at a constant heating rate.

3.1. Dynamic kinetics

We performed a kinetic analysis using two kinetic models: the Kissinger and Flynn–Wall–Ozawa models [12–14]. We used these two methods in this study rather than other non-isothermal methods because they do not require a prior knowledge of the reaction mechanism in order to quantify the kinetic parameters.

According to the Kissinger method, the activation energy is obtained from the maximum reaction rate where $d(d\alpha/dt)/dt$ is zero under condition of a constant heating rate. The resulting relation can be expressed as

$$\frac{d[\ln(q/T_m^2)]}{d(1/T_m)} = -\frac{E}{R} \tag{2}$$

where T_m is the temperature at which the rate is maximized and q is a constant heating rate. Therefore, a plot of $\ln(q/T_m^2)$ versus $1/T_m$ gives the activation energy without the need to make any assumptions about the conversion-dependent function.

Flynn–Wall–Ozawa developed an alternative method to calculate the activation energy, based on the equation:

$$\log(q) = \log\left[\frac{AE}{g(\alpha)R}\right] - 2.315 - \frac{0.457E}{RT} \tag{3}$$

Using this equation, a more accurate value of the activation energy can be obtained by iteration or least-squares techniques to improve the linear approximation of the temperature integration term.

Both the Kissinger and Flynn–Wall–Ozawa methods assume that the DSC peak exotherm is an iso-conversion and its value is independent of the heating rate. We employed these two methods in this study by using the data obtained in the dynamic heating experiments at different heating rates between 10 and 40 °C min^{-1}. Fig. 1 displays the heat flow measured by DSC during curing at various heating rates. The temperature of maximum rate (T_p) increases from 154.0 to 206.2 °C upon increasing the heating rate.

By applying the Flynn–Wall–Ozawa and Kissinger methods to the observed maximum reaction rate (i.e. the peak of the DSC thermogram), we determined the activation energy from the slope of the line presented in Fig. 2. The calculated activation energies for curing of the OG/mPDA system are 49.21 and 51.95 kJ/mol according to the Kissinger and Flynn–Wall–Ozawa methods, respectively. The corresponding activation energies obtained for curing of the DGEBA/mPDA are 48.21 and 48.33 kJ/mol, respectively. Therefore, the OG/mPDA system has a slightly higher activation energy than that of the DGEBA/mPDA, implying that OG has lower reactivity than DGEBA.

3.2. Isothermal kinetics

The conversion and the rate of conversion proceed continuously through the reaction as the uncured resin is cured isothermally. The conversion is measured using

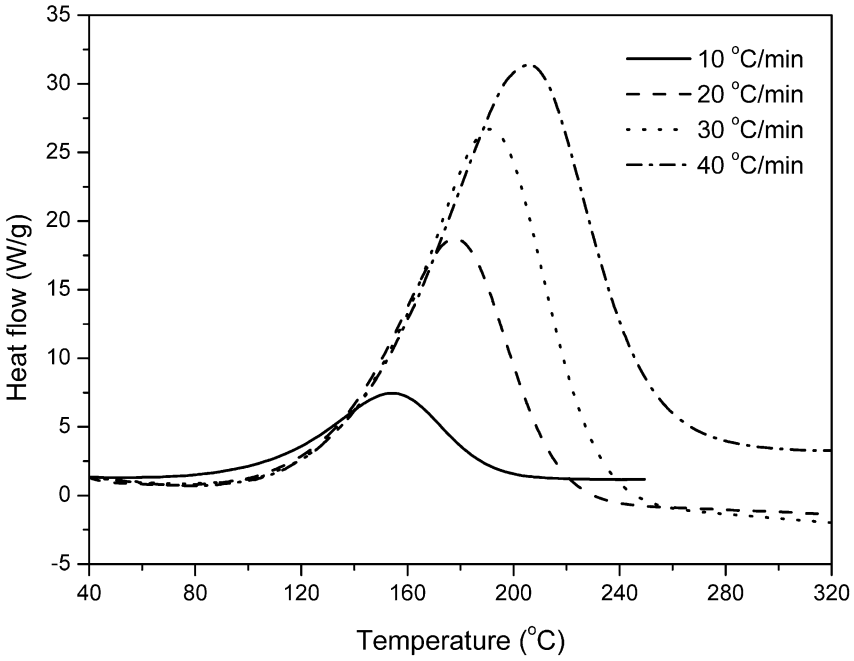

Fig. 1. Typical dynamic DSC thermograms of the OG/mPDA system.

DSC as

$$\alpha_t = \frac{\Delta H_h}{\Delta H_{Rxn}} \tag{4}$$

where the subscript t indicates the value at time t and ΔH_h is the heat of reaction at time t. An alternative method is to measure the heat evolved during cross-linking of the partially cured sample. This latter method becomes necessary when the exothermic energy is too small to be detected by the former method. A distinct advantage of the latter method is that it allows the value of T_g and the conversion to be measured simultaneously. With this method, the percentage conversion is calculated using the equation

$$\alpha_t = \frac{\Delta H_{Rxn} - \Delta H_r}{\Delta H_{Rxn}} \tag{5}$$

where ΔH_r is the residual heat of reaction. The analysis of autocatalyzed curing reactions assumes that at least one of the reaction products is also involved in the propagation reaction characterized by an accelerating isothermal conversion rate. The kinetics of autocatalyzed reactions are

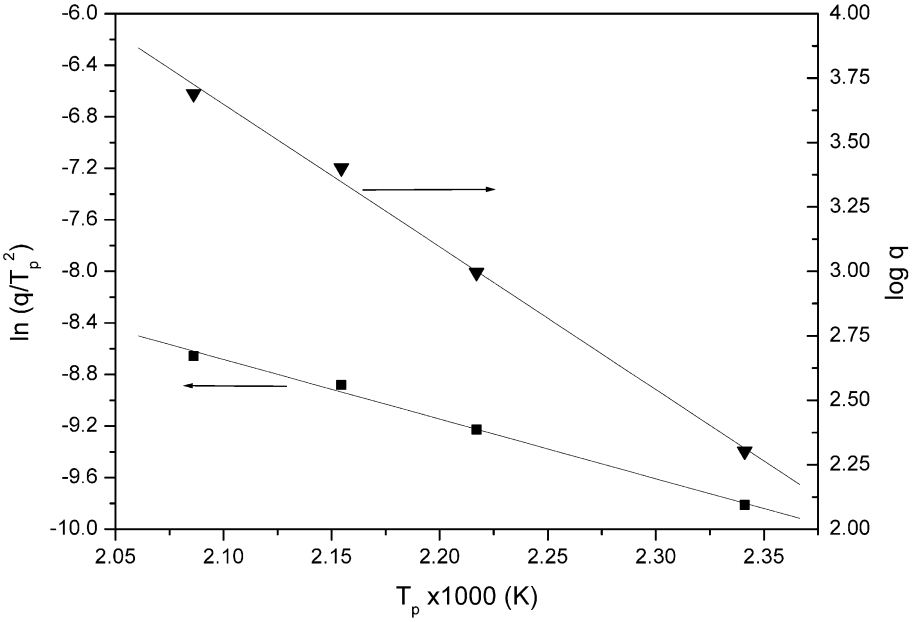

Fig. 2. Activation energies for the curing of the OG/mPDA system obtained by the Kissinger method and Flynn–Wall–Ozawa methods.

described as follows

$$\frac{d\alpha}{dt} = k'\alpha^m(1-\alpha)^n \quad (6)$$

where $m$is reaction order of autocatalytic reaction and n is reaction order of nonautocatalytic reaction and $k'(T)$ is the specific rate constant.

Fig. 3 displays typical isothermal DSC thermograms of the OG/mPDA system. The peaks indicating the times at which the reaction rates reach their maxim at curing temperatures of 90, 100, 110 and 120 °C occurring at 15.79, 5.68, 4.04and 1.98 min, respectively. The reaction rate at any temperature increases with time and passes through a maximum. The maximum reaction peak has a higher intensity, and less time is needed as the isothermal temperature is increased. Fig. 4 displays plots of the reaction rate versus conversion for the OG/mPDA system where maximum rates are reached at conversions between 0.2 and 0.4 (Table 1).

The findings in Fig. 4 indicate that the curing reaction of the OG/mPDA system is autocatalytic in nature and, thus, Eq. (6) is applicable. Table 2 lists the kinetic parameters obtained for OG cured with mPDA. The activation energies of the isothermal kinetics of the OG/mPDA and DGEBA/mPDA systems are 59.11 and 53.5 kJ/mol [15], similar trend occurs here as they did for the dynamic kinetics study.

3.3. Curing process

We characterized the curing process of the DGEBA/mPDA and OG/mPDA systems by FTIR spectroscopy at both 120 and 190 °C. Fig. 5 displays the FTIR spectra obtained at various time periods during the curing process of the DGEBA/mPDA (A) and OG/mPDA (B) systems by heating at 120 °C (pre-cured) and 190 °C (post-cured), respectively. A comparison of the spectra for the curing process at 120 °C reveals that the stretching vibration band of the epoxy ring at 910 cm^{-1} decreases upon increasing the curing time. Both systems were then heated at 190 °C for 180 min of the post-cured process. After post-curing, the epoxy characteristic peak (910 cm^{-1}) of the DGBEA/mPDA system is almost disappeared. In the OG/mPDA system, substantial fraction of unreacted epoxy peak still present. Fig. 6 displays the epoxy conversion based on $A_{910\ cm^{-1}}/A_{829\ cm^{-1}}$ at various time periods during the curing process of DGEBA/mPDA (A) and OG/mPDA (B) systems by heating at 120 °C (pre-cured). The $A_{910\ cm^{-1}}$ is the area of epoxy ring and $A_{829\ cm^{-1}}$ is area of the phenyl group of

Table 1
Temperatures of the peaks of the exotherms and the corresponding activation energies, obtained from DSC analysis during curing of the OG/mPDA and DGEBA/mPDA systems

q (°C/min)		T_p^1 (°C)	
		OG/mPDA	DGEBA/mPDA
10		154.0	150.4
20		177.9	174.2
30		191.0	184.0
40		206.2	200.2
E_a (kJ/mol)	Kissinger	49.21	45.21
	Flynn–Wall–Ozawa	51.95	48.33

T_p^1: the temperature of maximum rate.

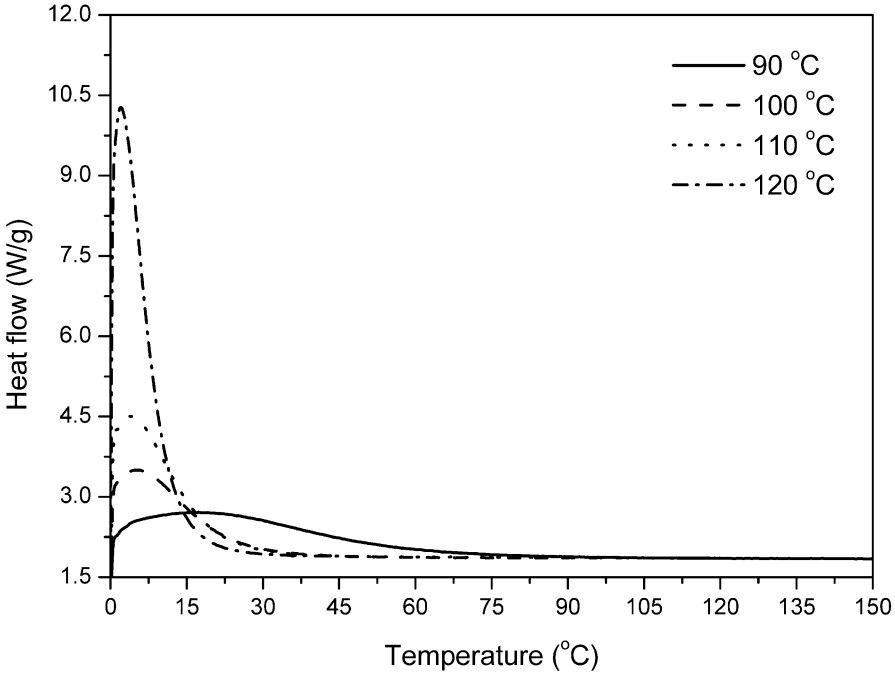

Fig. 3. Typical isothermal DSC thermograms of the OG/mPDA systemat various curing temperatures.

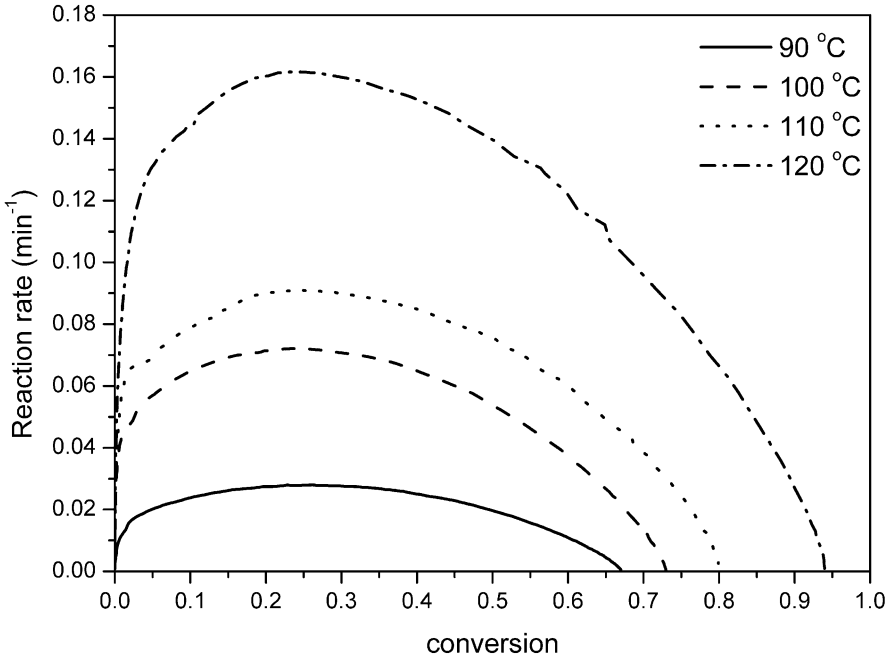

Fig. 4. Reaction rate versus conversion of the OG/mPDA system at various curing temperatures.

mPDA. The DGEBA/mPDA has the usual high conversion as would be expected. Due to the severe steric effect of the POSS units of the OG monomer of OG/mPDA system results in incomplete curing only 50% epoxy conversion after pre-curing.

3.4. Curing mechanism of OG/mPDA system

We confirmed the curing mechanism of OG/mPDA by FTIR spectroscopy and ^{13}C NMR and ^{13}C solid state NMR. Fig. 7 displayed the chemical shifts of ^{13}C NMR of OG for $-CH_3$ group at -0.5 ppm and epoxy group at 50.6 and 44.0 ppm. Fig. 8 displayed the chemical shifts of mPDA for meta-diamine phenyl group at 147.3 ppm. Fig. 9 showed the chemical shifts of ^{13}C solid state NMR of OG cured with mPDA for $-CH_3$ group of OG at -0.4 ppm, epoxy group at 53.2 and 46.4 ppm, and meta-diamine phenyl group of mPDA at 145.5 ppm and other chemical shifts of OG cured with mPDA were exist in NMR spectra. Fig. 5 showed the FTIR spectra obtained at various time periods during the curing process of the OG/mPDA (B) system and the FTIR spectra showed the unreacted epoxy group at 910 cm^{-1} and the epoxy group conversion is 50%. Scheme 3 showed the curing mechanism for OG/mPDA system.

3.5. Glass transition temperature

Modulated differential scanning calorimetry (MDSC) was applied to determine the glass transition temperature (T_g) of the post-cured epoxies. Fig. 10 displays the thermograms of reverse heat flow versus temperature of the OG/mPDA and DGEBA/mPDA systems and results are summarized in Table 3. Fig. 10 shows the glass transition of OG/mPDA system is less clearly defined due to the POSS cluster slows down the transition from glasslike behavior to rubberlike behavior [16]. The values of T_g of OG/mPDA and DGEBA/mPDA systems are at 239.3 and 159.5 °C, respectively. In literatures [6,16,17] had been reported that the presence of the rigid POSS cages is able to effectively hinder the motion of the network junctions even the epoxy conversion is very lower. Due to the POSS clusters nanoscopic size, hinder the motion of network junctions. Therefore, the T_g of the OG/mPDA network is substantially higher than that of the DGEBA/mPDA network [5,8,10].

Table 2
Data obtained during isothermal curing of OG/mPDA system at various curing temperatures

Curing temperature (°C)	Rate constant (min^{-1})	Reaction order		E_a^1 (kJ/mol)
		m	*n*	
90	0.0454	0.35	0.90	59.11
100	0.108	0.27	0.92	
110	0.125	0.24	0.89	
120	0.229	0.24	0.96	

E_a^1: the activation energy of curing reaction.

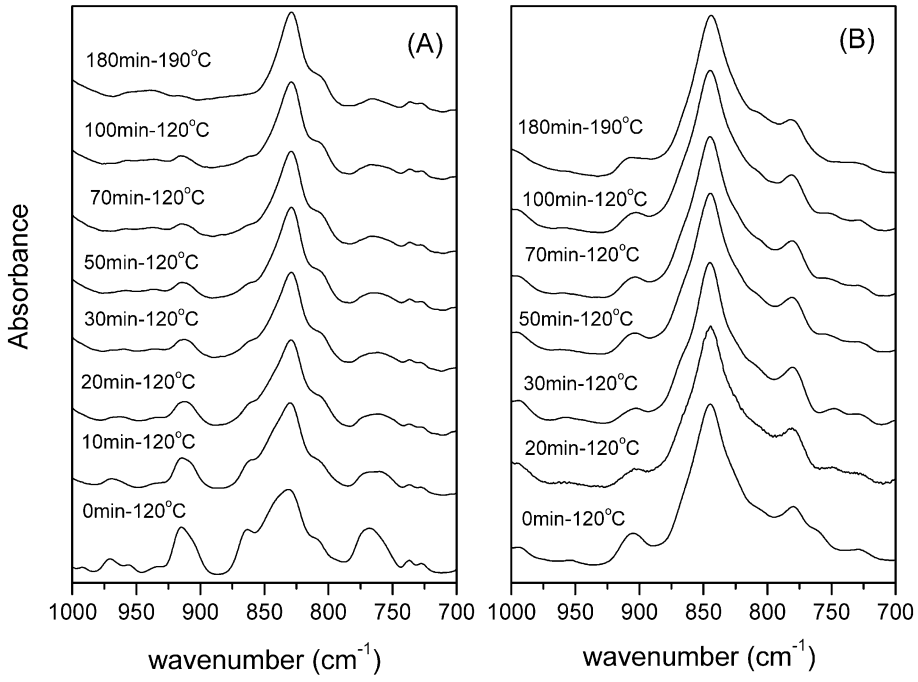

Fig. 5. FTIR spectra obtained during the process of curing (A) DAEBA/mPDA (B) OG/mPDA.

Table 3
Thermal properties and dielectric constant of OG/mPDA and DGEBA/mPDA materials

	T_g (°C)	$T_{d,init}$ (°C)	$T_{d,max}$ (°C)	DTG (%/min)	Char yield at 750 °C (%)	Dielectric constant
OG/mPDA	239	254	439	15.8	38.8	2.31
DGEBA/mPDA	160	345	385	47.8	14.2	3.51

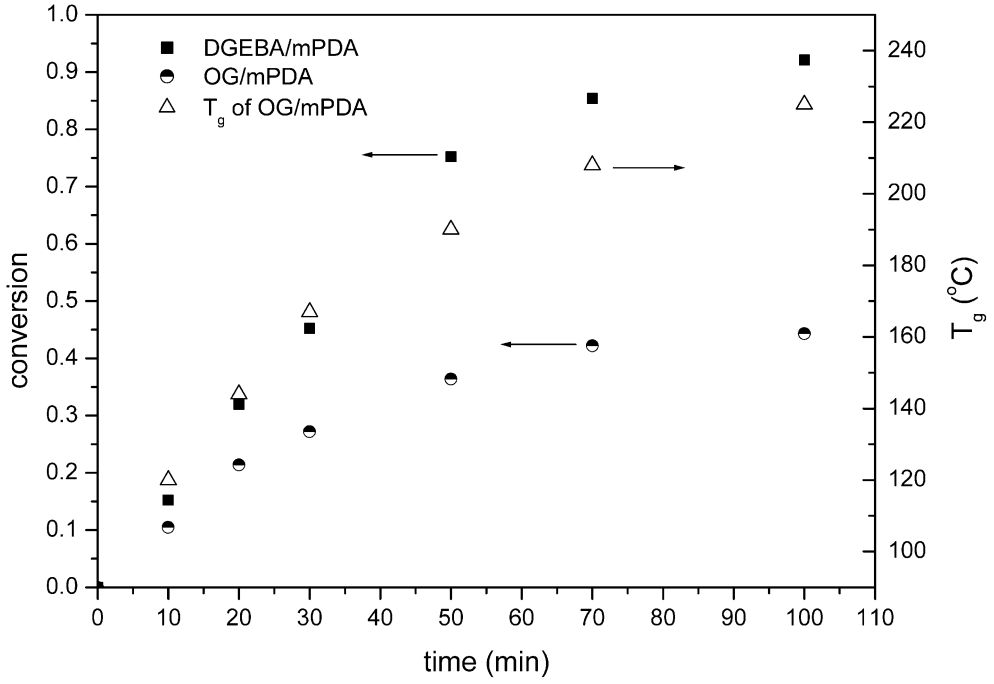

Fig. 6. Plot of conversion of epoxy ring during the process of curing (A) DAEBA/mPDA (B) OG/mPDA.

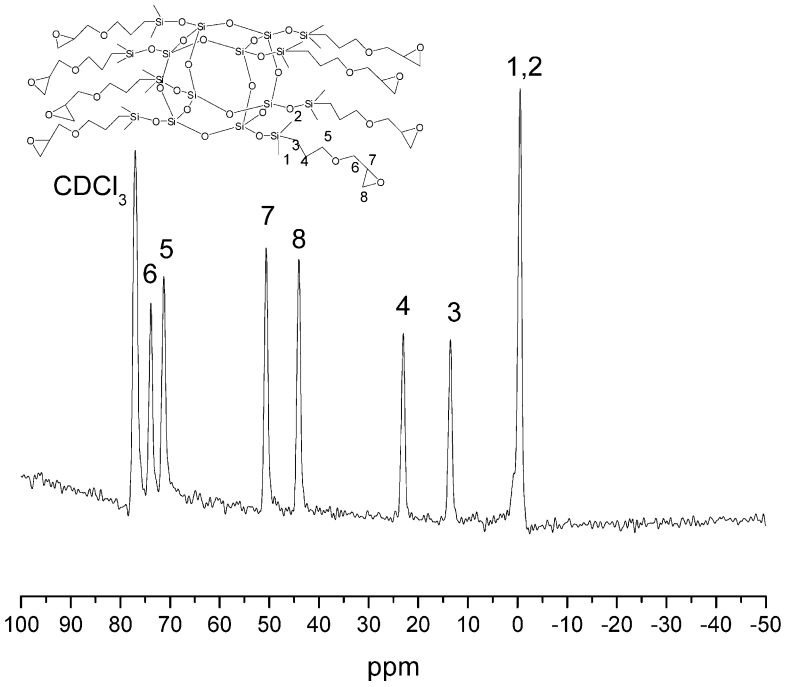

Fig. 7. ^{13}C NMR spectrum of OG.

Fig. 11 showed the thermogram of tan δ of DMA of OG/mPDA at frequency = 1 and temperature of α-relaxation (T_g) is at 235 °C (closely to MDSC result). Fig. 6 showed the epoxy conversion verse T_g of OG/mPDA and observed that the T_g of OG/mPDA increased with epoxy conversion increasing. Due to the T_g increased with crosslinking density increasing and the crosslinking density increased with epoxy conversion increasing.

3.6. Thermal stability

The TGA thermograms of the post-cured OG/mPDA and DGEBA/mPDA under N_2 atmosphere are presented in Fig. 8 and results are summarized in Table 3. The initial decomposition temperature ($T_{d,init}$) of the OG/mPDA (254 °C) is lower than that of the DGEBA/mPDA (345 °C). As indicated in Fig. 5, a significant fraction of

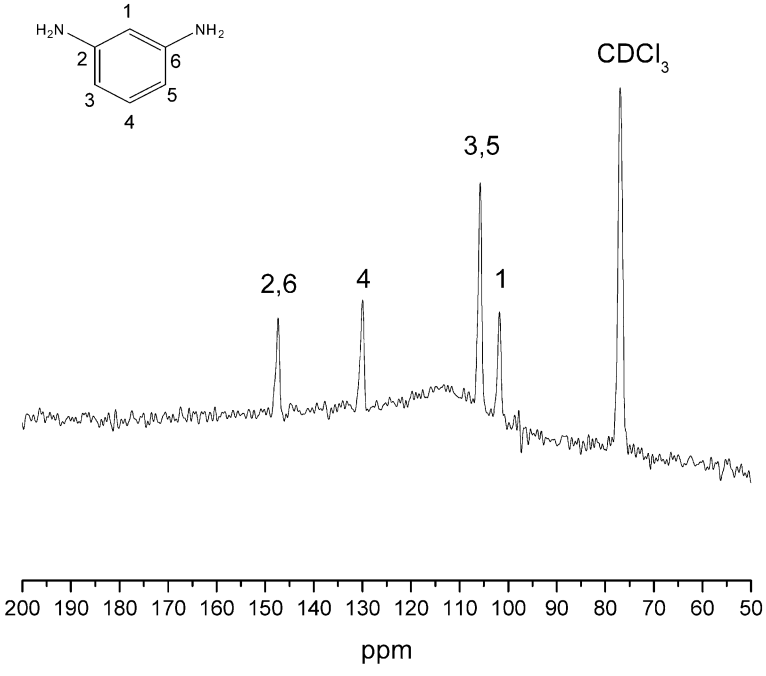

Fig. 8. ^{13}C NMR spectrum of mPDA.

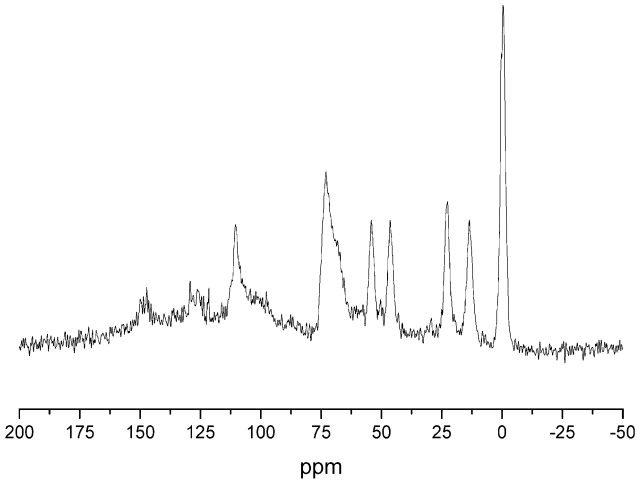

Fig. 9. ^{13}C solid state NMR spectrum of OG cured with mPDA.

unreacted epoxy (~50%) still exists in the FTIR spectrum of the post-cure product. Therefore a similar mole fraction of unreacted amino groups is also expected to be present because stoichiometric quantities of epoxy and amino are employed in preparing this OG/mPDA system. Amino groups that are either pendent or unreacted in the final cured product tend to decompose or volatilize upon heating at relatively low temperatures [6]. Therefore, the value of $T_{d,init}$ of the OG/mPDA material lower than that of DGEBA/mPDA understandable. However, maximum decomposition rate temperature ($T_{d,max}$) of the former is higher than the latter (439 °C versus 385 °C). Maximum decomposition rate ($DTG_{,max}$) of the former is lower than the latter (15.8%/min versus 47.8%/min). Because the cage structure of the OG/mPDA is more stable. The char yield at 750 °C of the OG/mPDA system is also significantly higher than that of the DGEBA/mPDA (38.8 versus 14.2%). This result can be interpreted as the consequence of degradation of the POSS structure to form SiO_2 that is inflammable [6,17]. In conclusion, the OG/mPDA should inherently possess higher thermal stability than the DGEBA/mPDA, however, the presence of unreacted amine group causes lower initial decomposition temperature (Fig. 12).

3.7. Dielectric constant

We characterized the dielectric constant of cured OG/mPDA and DGEBA/mPDA by DEA and density test. For DEA testing, dielectric constants of the finally cured OG/mPDA and DGEBA/mPDA materials at 100 kHz and 25 °C are 2.31 and 3.51, respectively (Table 3). For density testing, the results were shown in Table 4 and the density of OG/mPDA system was lower than DGEBA/mPDA and OG/mPDA system had high porosity (24%). It has been reported previously that higher POSS content results in a lower dielectric constant [18]. Thus, as expected, the POSS-containing OG/mPDA system possesses a lower dielectric constant than that of the DGEBA/mPDA system. The presence of nanoporous cubes-like POSS units in the epoxy resin is responsible for the lower dielectric constant [18,19].

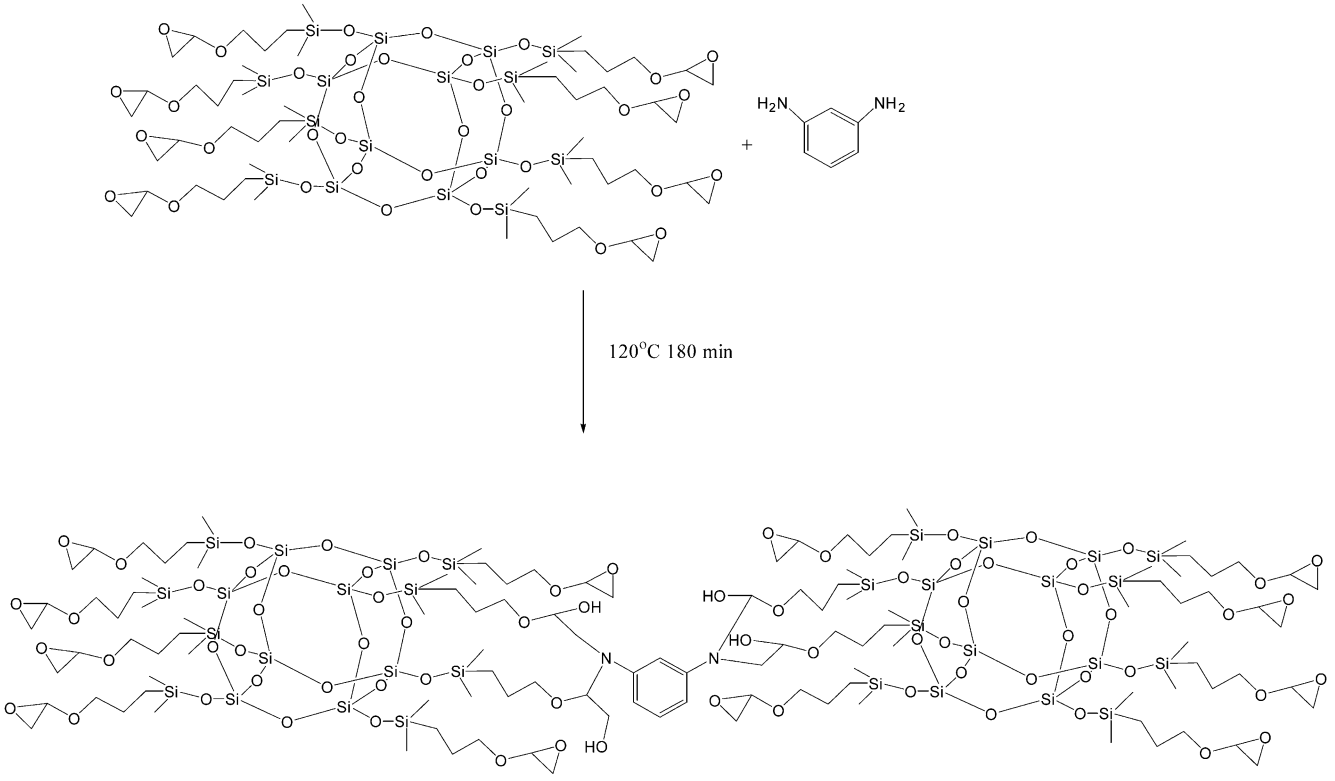

Scheme 3. Curing mechanism of OG cured with mPDA.

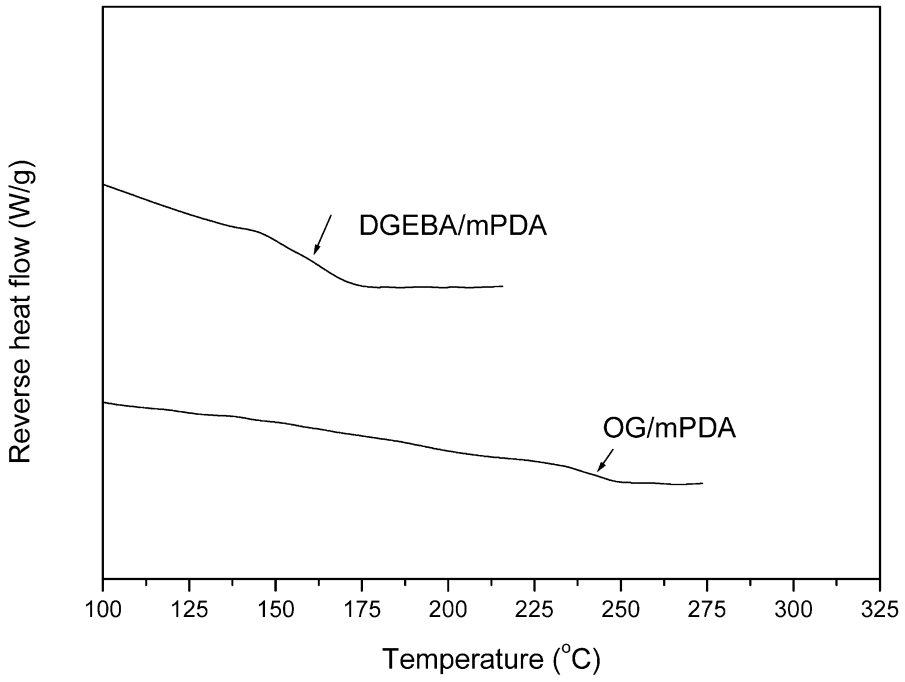

Fig. 10. Plot of reverse heat flow versus temperature obtained during MDSC analysis of the OG/mPDA and DGEBA/mPDA systems.

Table 4
Densities of OG/mPDA and DGEBA/mPDA systems

	Theoretical density (g/cm^3)	Measured density (g/cm^3)	Porosity (%)	Fraction free volume* (FFV)
DGEBA/mPDA	1.38	1.34	0	0.29
OG/mPDA	1.30	1.02	24	0.51

Fraction Free volume*: fractional free volume

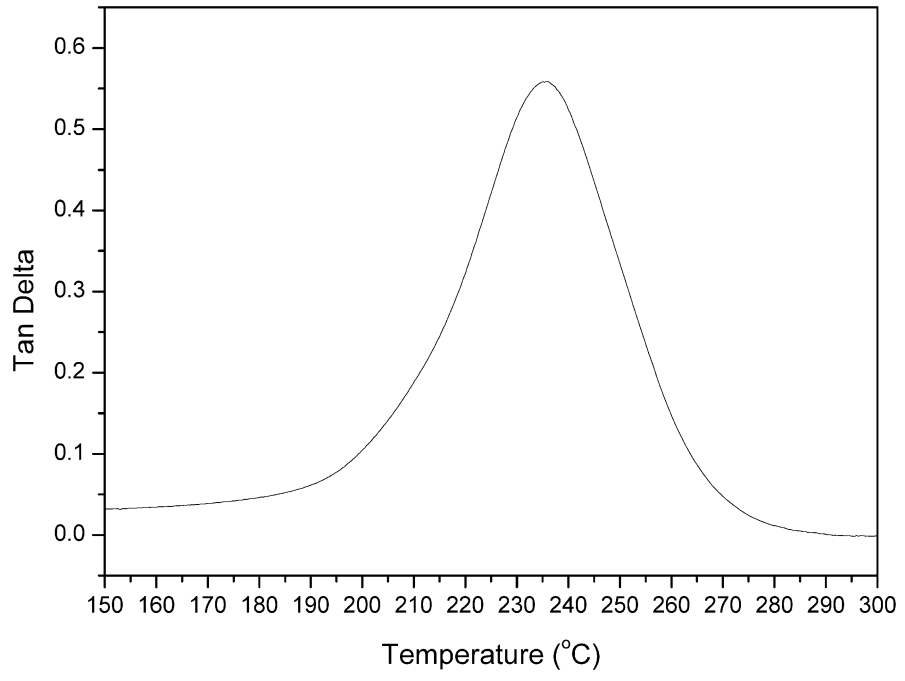

Fig. 11. Thermogram of tan δ of DMA of OG/mPDA.

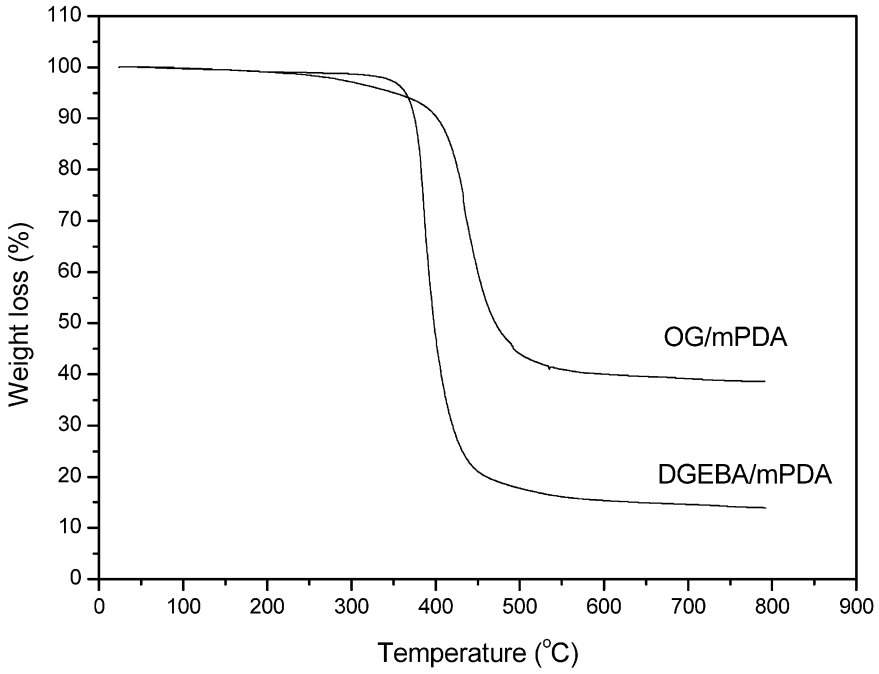

Fig. 12. TGA thermograms of OG/mPDA and DGEBA/mPDA materials.

4. Conclusions

A new nanomaterial based on POSS-epoxy (OG) and meta-phenylenediamne (mPDA) has been synthesized. The activation energy in curing OG/mPDA system is higher than that of DGEBA/mPDA system based on both Kissinger and Flynn–Wall–Ozawa methods. In an isothermal kinetic study based on autocatalytic system, the activation energy for curing OG/mPDA is also higher than that of the DGEBA/mPDA system. The glass transition temperature (T_g) of the cured OG/mPDA product is significantly higher than that of the DGEBA/mPDA material due to the presence of the POSS cages that is able to effectively hinder the motion of the network junctions. The cured OG/mPDA product inherently possesses higher thermal stability than the cured DGEBA/mPDA product based on higher maximum decomposition rate temperature, and higher char yield of the former. However, the existence of large fraction of the unreacted amine groups causes lower initial decomposition temperature of the OG/mPDA because it tends to decompose or volatilize on heating at relatively low temperature. The dielectric constant of the OG/mPDA material (2.31) is substantially lower than that of the DGEBA/mPDA (3.51) as a consequence the presence of nanoporous POSS cubes in the epoxy matrix.

References

[1] Lichtenhan JD, Otonari YA, Carr MJ. Macromolecules 1995;28:8435.
[2] Pyun J, Matyjaszewski K. Macromolecules 2000;33:217.
[3] Haddad TS, ichtenhan JD. Macromolecules 1996;29:7302.
[4] Math PT, Jeon HG, Romo-Uribe A, Haddad TS, Lichtenhan JD. Macromolecules 1999;32:1194.
[5] Lee A, Lichtenhan JD. Macromolecules 1998;31:4970.
[6] Jiwon C, Jason H, Albert FY, Quan Z, Richard ML. J Am Chem Soc 2001;123:11420.
[7] Maria JA, Luis B, Diana PF, Roberto JJW. Macromolecules 2003;36:3128.
[8] Li GZ, Wang L, Toghiani H, Daulton Jr TL, Pittman CU. Polymer 2002;43:4167.
[9] Ramirez C, Abad MJ, Barral L, Cano J, Diez FJ, Lopez J, Montes R, Polo J. J Therm Analy Calor 2003;72:421.
[10] Li GZ, Wang L, Ni HL, Charles Pittman Jr. CU. J Inorg Organometal Polym 2001;11:123.
[11] Boey FYC, Qiang W. Polymer 2000;41:2081.
[12] Kissinger HE. Anal Chem 1957;29:1702.
[13] Flynn JH, Wall LA. J Res Nat Bur Stand Part: A Phys Chem 1996;70A:487.
[14] Ozawa T. Bull Chem Soc Jpn 1965;38:1881.
[15] Zevtkov VL. Polymer 2002;43:1069.
[16] Lee A, Lichtenhan JD. J Appl Polym Sci 1999;73:1993.
[17] Choi J, Kim SG, Laine RM. Macromolecules 2004;37:99.
[18] Leu CM, Chang YT, Wei KH. Chem Mater 2003;15:3721.
[19] Leu CM, Reddy GM, Wei KH, Shu CF. Chem Mater 2003;15:2261.